# Supplemental Information

## Supplemental Figures

### Figure S1

**a**

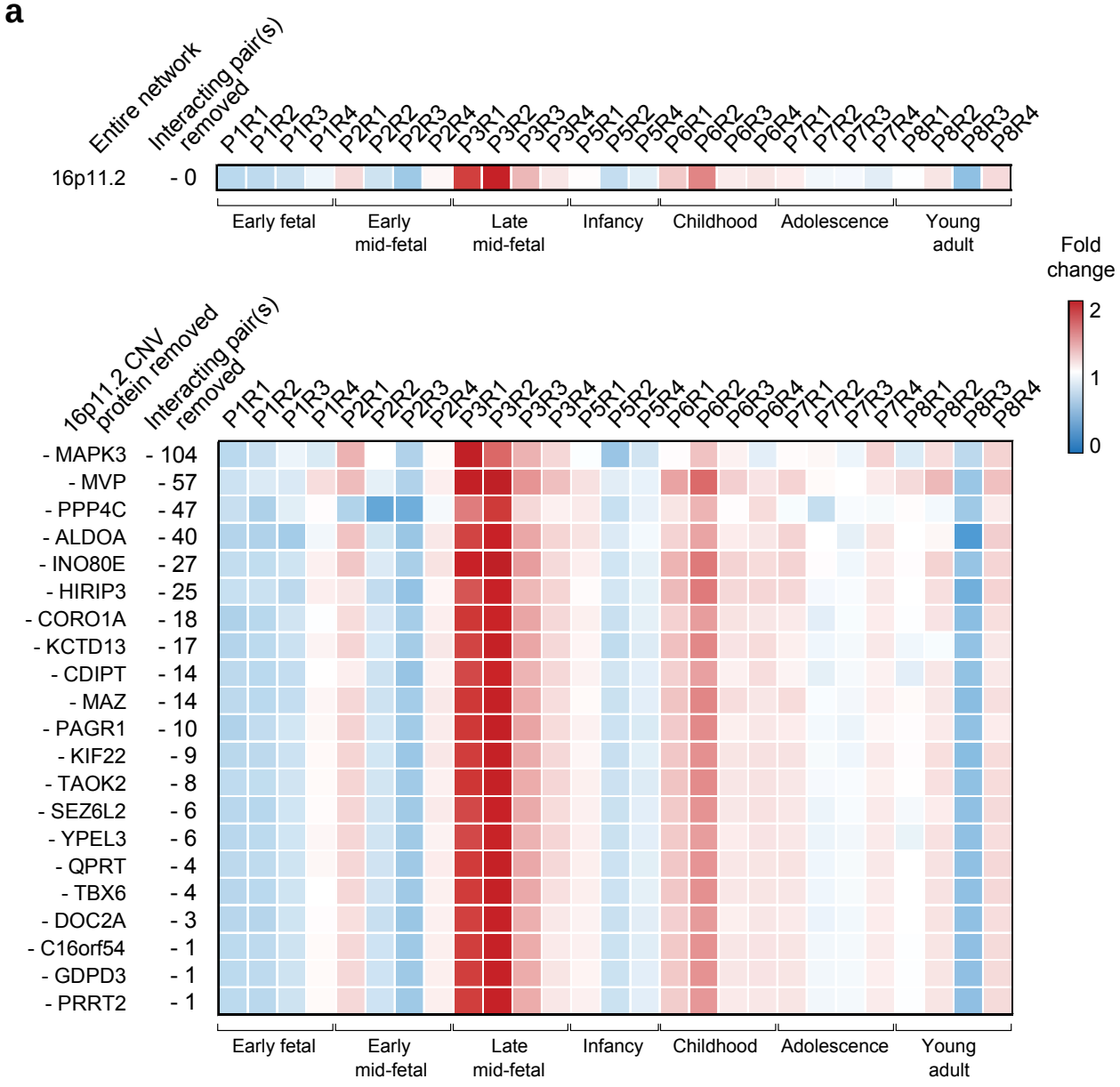

**b**

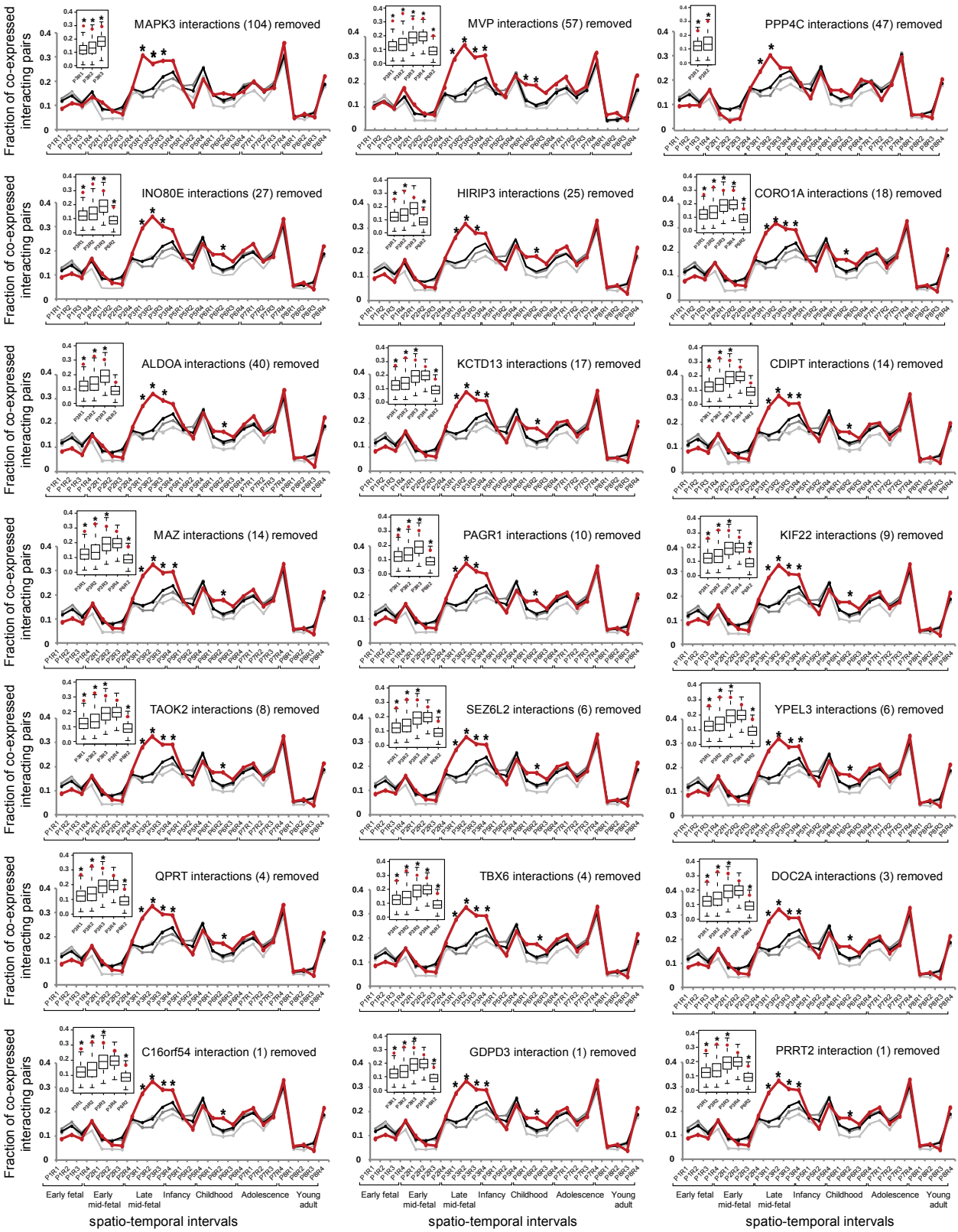
MAPK3 interactions (104) removed
MVP interactions (57) removed
PPP4C interactions (47) removed
INO80E interactions (27) removed
HIRIP3 interactions (25) removed
CORO1A interactions (18) removed
ALDOA interactions (40) removed
KCTD13 interactions (17) removed
CDIPT interactions (14) removed
MAZ interactions (14) removed
PAGR1 interactions (10) removed
KIF22 interactions (9) removed
TAOK2 interactions (8) removed
SEZ6L2 interactions (6) removed
YPEL3 interactions (6) removed
QPRT interactions (4) removed
TBX6 interactions (4) removed
DOC2A interactions (3) removed
C16orf54 interaction (1) removed
GDPD3 interaction (1) removed
PRRT2 interaction (1) removed
Fraction of co-expressed interacting pairs
Early fetal
Early mid-fetal
Late mid-fetal
Infancy
Childhood
Adolescence
Young adult
spatio-temporal intervals

## Figure S2

**a**

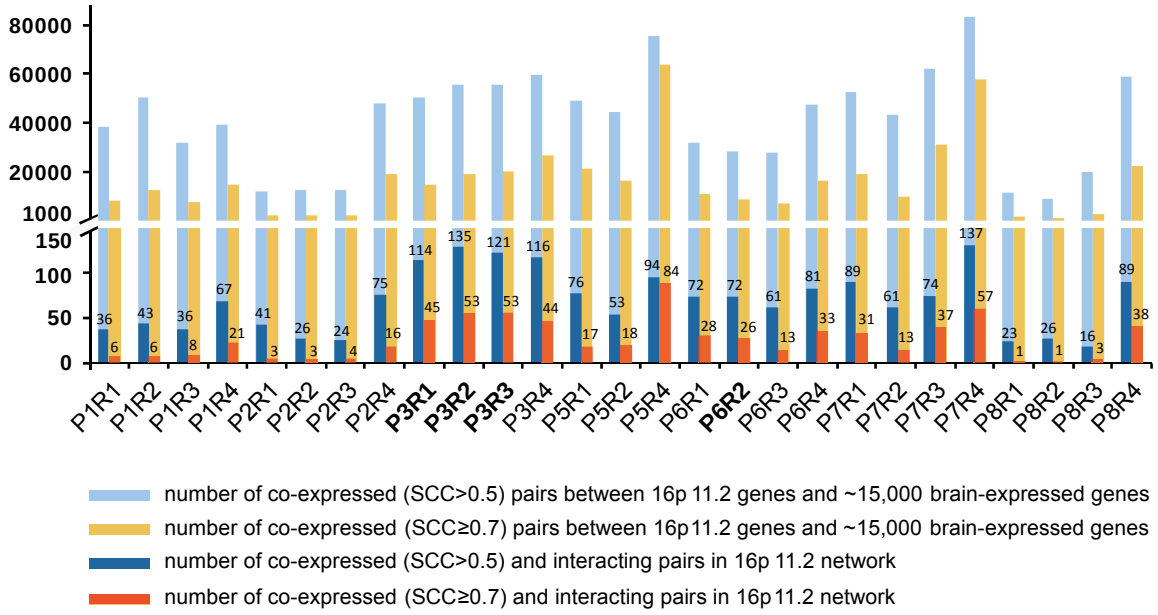
80000
60000
40000
20000
1000
150
100
50
0
P1R1 P1R2 P1R3 P1R4 P2R1 P2R2 P2R3 P2R4 P3R1 P3R2 P3R3 P3R4 P5R1 P5R2 P5R4 P6R1 P6R2 P6R3 P6R4 P7R1 P7R2 P7R3 P7R4 P8R1 P8R2 P8R3 P8R4
number of co-expressed (SCC>0.5) pairs between 16p 11.2 genes and ~15,000 brain-expressed genes
number of co-expressed (SCC≥0.7) pairs between 16p11.2 genes and ~15,000 brain-expressed genes
number of co-expressed (SCC>0.5) and interacting pairs in 16p 11.2 network
number of co-expressed (SCC≥0.7) and interacting pairs in 16p11.2 network

**b**

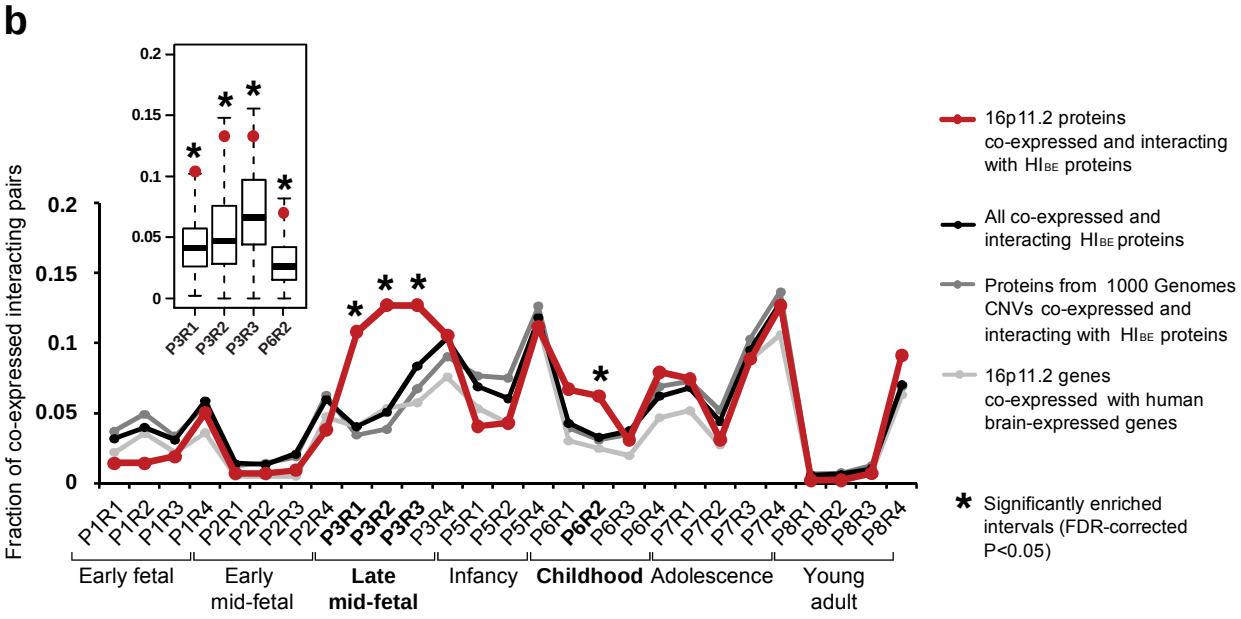
Fraction of co-expressed interacting pairs
0.2
0.15
0.1
0.05
0
P3R1 P3R2 P3R3 P6R2
Early fetal
Early mid-fetal
Late mid-fetal
Infancy
Childhood
Adolescence
Young adult
16p11.2 proteins co-expressed and interacting with HIBE proteins
All co-expressed and interacting HIBE proteins
Proteins from 1000 Genomes CNVs co-expressed and interacting with HIBE proteins
16p11.2 genes co-expressed with human brain-expressed genes
* Significantly enriched intervals (FDR-corrected P<0.05)

## Figure S3

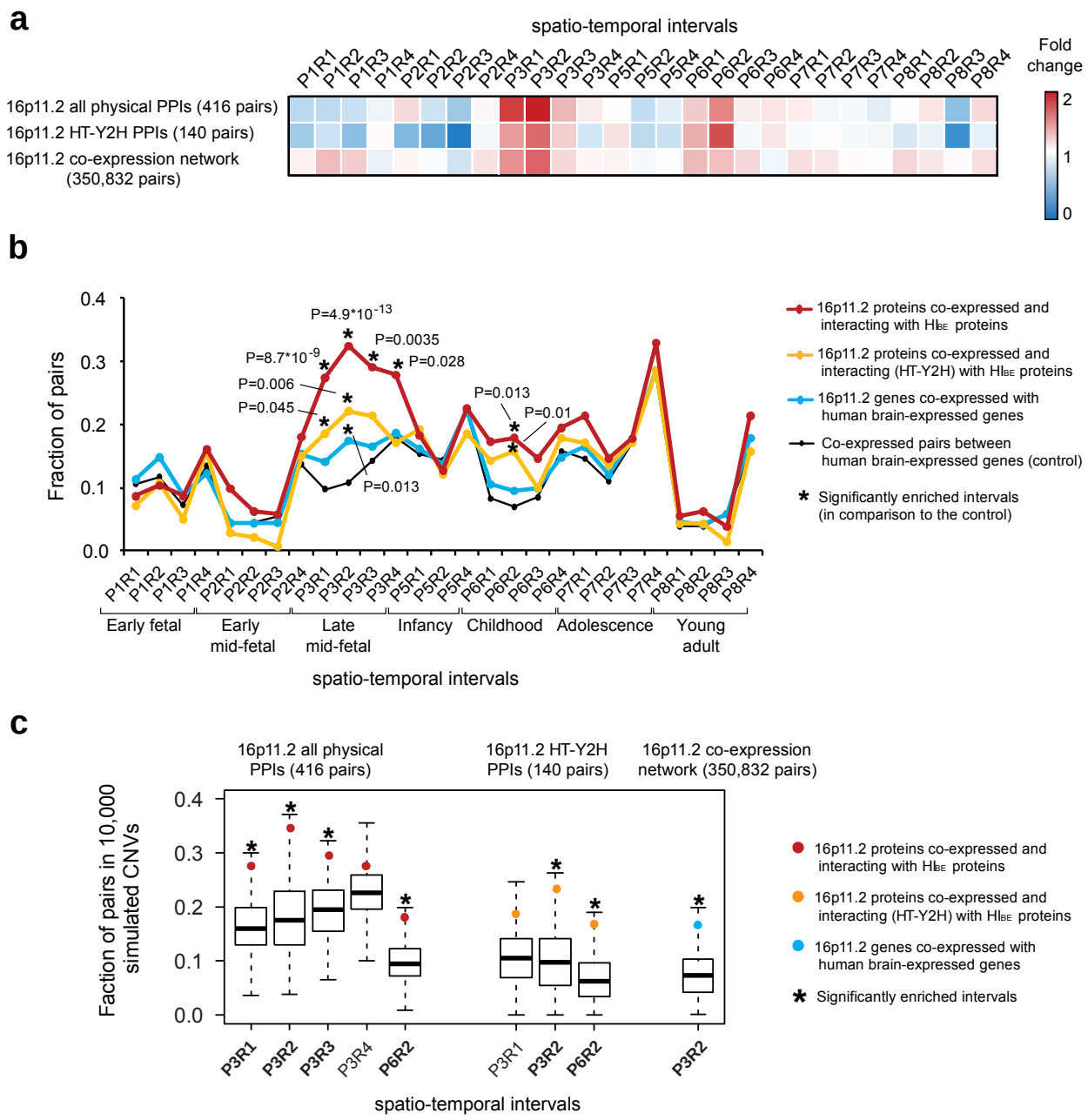
a
spatio-temporal intervals
P1R1 P1R2 P1R3 P1R4 P2R1 P2R2 P2R3 P2R4 P3R1 P3R2 P3R3 P3R4 P5R1 P5R2 P5R4 P6R1 P6R2 P6R3 P6R4 P7R1 P7R2 P7R3 P7R4 P8R1 P8R2 P8R3 P8R4
16p11.2 all physical PPIs (416 pairs)
16p11.2 HT-Y2H PPIs (140 pairs)
16p11.2 co-expression network (350,832 pairs)
Fold change
2
1
0
b
Fraction of pairs
0.4
0.3
0.2
0.1
0.0
P=4.9*10-13
P=0.0035
P=8.7*10-9
P=0.028
P=0.006
P=0.045
P=0.013
P=0.01
P=0.013
Early fetal
Early mid-fetal
Late mid-fetal
Infancy
Childhood
Adolescence
Young adult
spatio-temporal intervals
16p11.2 proteins co-expressed and interacting with HIBE proteins
16p11.2 proteins co-expressed and interacting (HT-Y2H) with HIBE proteins
16p11.2 genes co-expressed with human brain-expressed genes
Co-expressed pairs between human brain-expressed genes (control)
* Significantly enriched intervals (in comparison to the control)
c
16p11.2 all physical PPIs (416 pairs)
16p11.2 HT-Y2H PPIs (140 pairs)
16p11.2 co-expression network (350,832 pairs)
Faction of pairs in 10,000 simulated CNVs
0.4
0.3
0.2
0.1
0.0
P3R1 P3R2 P3R3 P3R4 P6R2 P3R1 P3R2 P6R2 P3R2
spatio-temporal intervals
16p11.2 proteins co-expressed and interacting with HIBE proteins
16p11.2 proteins co-expressed and interacting (HT-Y2H) with HIBE proteins
16p11.2 genes co-expressed with human brain-expressed genes
* Significantly enriched intervals

**Figure S4**

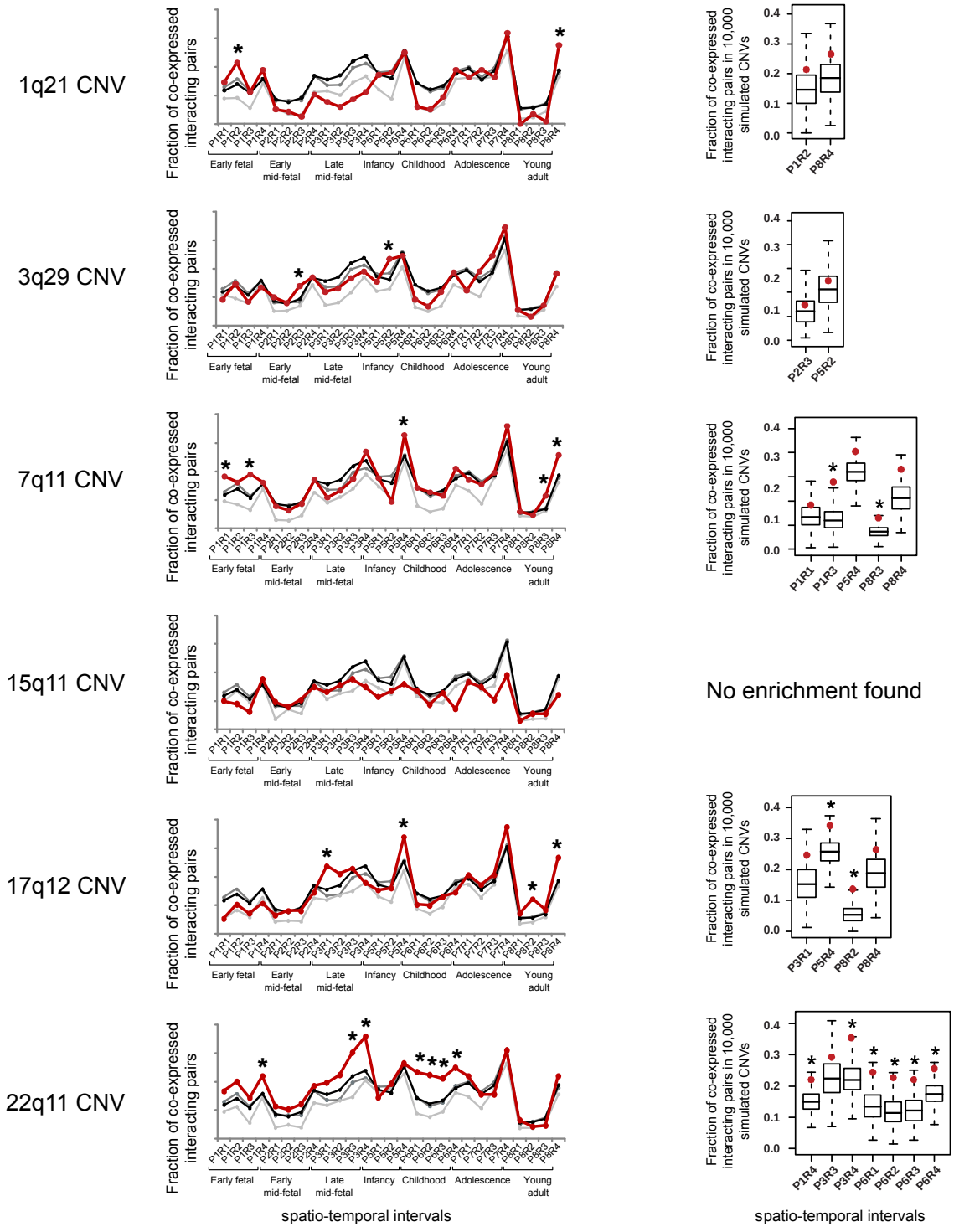


- CNV proteins co-expressed and interacting with $HI_{BE}$ proteins
- All co-expressed and interacting $HI_{BE}$ proteins
- 16p11.2 proteins co-expressed and interacting with $HI_{BE}$ proteins
- Proteins from 1000 Genomes CNVs co-expressed and interacting with $HI_{BE}$ proteins
- 16p11.2 genes co-expressed with human brain-expressed genes
- * Significantly enriched intervals
- * Significantly enriched intervals in comparison to at least 2 controls

## Figure S5

**a**

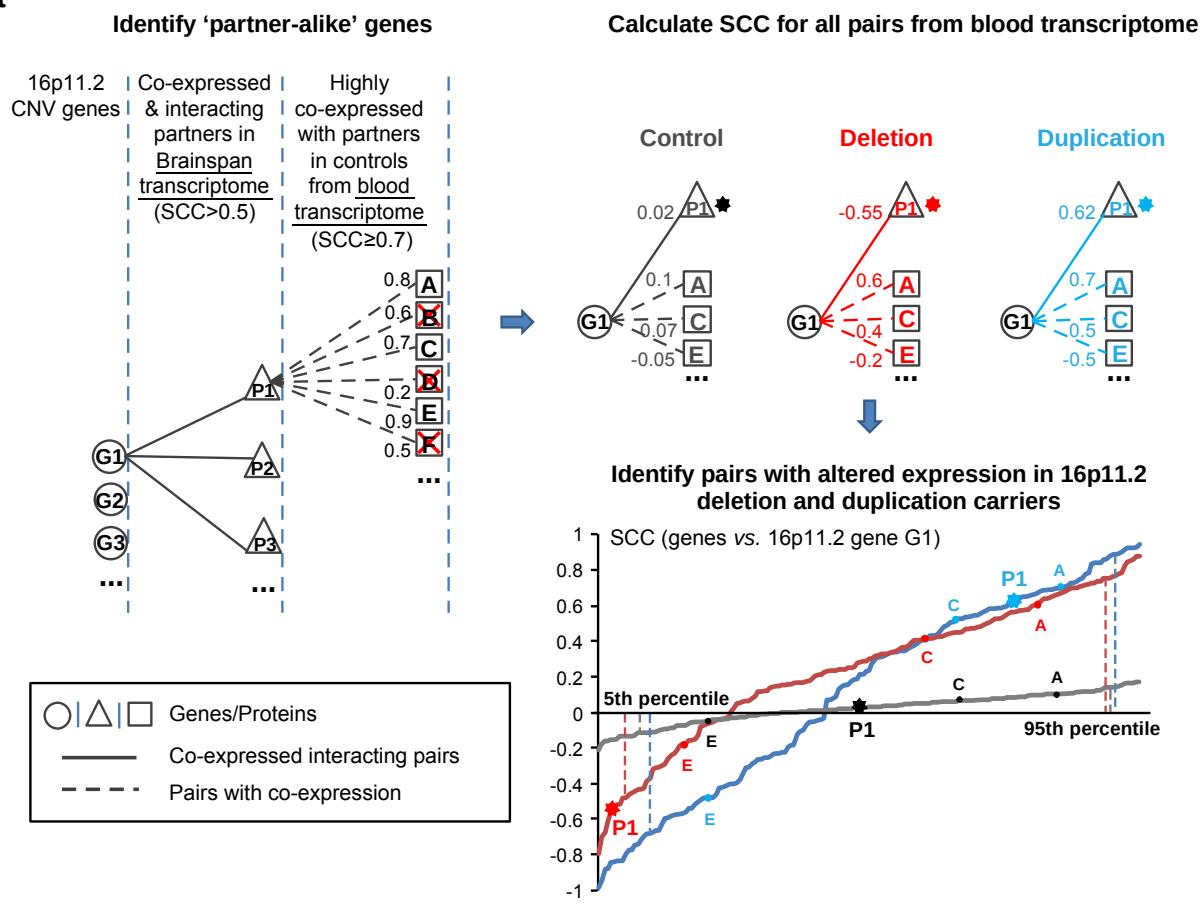
Identify 'partner-alike' genes
Calculate SCC for all pairs from blood transcriptome
16p11.2 CNV genes
Co-expressed & interacting partners in Brainspan transcriptome (SCC>0.5)
Highly co-expressed with partners in controls from blood transcriptome (SCC≥0.7)
Control
Deletion
Duplication
Identify pairs with altered expression in 16p11.2 deletion and duplication carriers
SCC (genes vs. 16p11.2 gene G1)
5th percentile
95th percentile
Genes/Proteins
Co-expressed interacting pairs
Pairs with co-expression

**b**

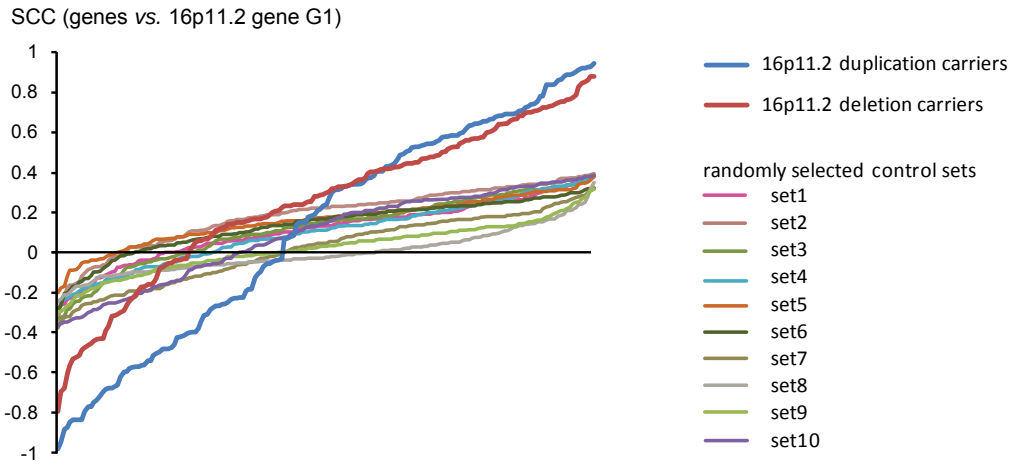
SCC (genes vs. 16p11.2 gene G1)
16p11.2 duplication carriers
16p11.2 deletion carriers
randomly selected control sets
set1
set2
set3
set4
set5
set6
set7
set8
set9
set10

## Supplemental Figure Legends

**Figure S1. The co-expressed interacting protein pairs removal test for 16p11.2 network, related to Figure 3. (a)** Each cell of the heatmap represents fold change of the fraction of co-expressed interacting protein pairs of the 16p11.2 CNV network compared with the background control of the co-expressed interacting protein pairs from the $HI_{BE}$ network. The fold change level ranges from 0 (blue) corresponding to depletion to 2 (red) corresponding to enrichment. **Upper panel:** the spatio-temporal signature of the 16p11.2 network. **Lower panel:** each row represents a signature observed after the removal of one 16p11.2 protein together with all of its interacting partners. The rows are sorted in the descending order of the number of interacting pairs removed from the network. The heatmap demonstrates that spatio-temporal 16p11.2 signature is not dependent on specific pairs and remains robust even after removal of a quarter (in the case of MAPK3) of all network pairs. **(b)** The fractions of protein pairs from the 16p11.2 CNV region co-expressed and interacting with $HI_{BE}$ proteins (red line), all co-expressed and interacting $HI_{BE}$ proteins (black line), proteins from 1000 Genome project CNVs co-expressed and interacting with $HI_{BE}$ proteins (dark grey line), and 16p11.2 CNV genes co-expressed with all brain-expressed human genes (light grey line) are shown. Twenty-seven spatio-temporal intervals of brain development are shown on the X-axis. Each graph represents enriched intervals (star symbols) after the removal of one 16p11.2 protein together with all of its interacting partners. The insets show spatio-temporal intervals with significant enrichment after correction against a background control of 10,000 simulated CNV networks with the same number of genes and interactions (±10%) as in the 16p11.2 network. The statistical enrichment was calculated using Fisher's exact test and P-values were FDR-corrected for multiple comparisons.

**Figure S2. Datasets comparison when using different co-expression thresholds, related to Figure 3. (a)** Comparison of the number of co-expressed pairs (light blue and yellow) with the

number of co-expressed interacting pairs (dark blue and red) at two Spearman correlation coefficient (SCC) thresholds, 0.5 and 0.7. Dramatic drop in the number of pairs is observed when PPIs are added to construct the network. For some of the spatio-temporal intervals the number of co-expressed interacting pairs (indicated above each column) drops to only one at the SCC≥0.7, decreasing our power to detect associations; **(b)** 16p11.2 network enrichment at the SCC≥0.7. Four spatio-temporal intervals remain significant.

**Figure S3. The co-expressed interacting protein pairs in 16p11.2 high-throughput Y2H (HT-Y2H) and co-expression only networks, related to Figure 3. (a)** Each cell of the heatmap represents fold change of the fraction of co-expressed interacting (or co-expressed only) pairs of the 16p11.2 CNV networks compared with the background control of the co-expressed interacting (or co-expressed only) pairs from $HI_{BE}$ network. The fold change level ranges from 0 (blue) corresponding to depletion to 2 (red) corresponding to enrichment. **Upper panel:** the spatio-temporal signature of the 16p11.2 network based on all 416 physical PPIs between 16p11.2 and $HI_{BE}$ proteins. **Middle panel:** the spatio-temporal signature of the 16p11.2 network based on 140 HT-Y2H physical PPIs between 16p11.2 and $HI_{BE}$ proteins. **Lower panel:** the spatio-temporal signature of the 16p11.2 network based on 350,832 co-expressed pairs between 16p11.2 and $HI_{BE}$ genes. **(b)** The fractions of pairs from the 16p11.2 CNV region co-expressed and interacting with $HI_{BE}$ proteins (red line), co-expressed and interacting (HT-Y2H PPIs only) with $HI_{BE}$ proteins (yellow line), co-expressed with $HI_{BE}$ genes (blue line), and co-expressed pairs between human brain-expressed genes (black line, control). The statistical enrichment was calculated using Fisher's exact test and P-values were FDR-corrected for multiple comparisons. **(c)** The spatio-temporal intervals with significant enrichment were further evaluated against a background control of 10,000 simulated CNV with the same number of genes and interactions as 16p11.2 CNV. P3R2 interval remained significant independently on the dataset used.

**Figure S4. Enrichment analyses of co-expressed interacting protein pairs from six high-risk CNVs, related to Discussion.** The enrichment profile of each CNV was compared to three control datasets (left column) and to 10,000 simulated CNV networks with the same number of genes and interactions (±10%) as in each CNV (right panel). No significantly enriched intervals have been found for 15q11 CNV, and the significant intervals for 1q21 and 3q29 did not withstand the stringent simulated CNV network correction. Statistically robust signatures were detected for three high-risk CNVs in addition to 16p11.2 *locus* (not shown).

**Figure S5. Overview of the method for identifying interacting pairs with altered expression in the 16p11.2 deletion and duplication carriers (based on Luo *et al.* blood transcriptome data), related to Discussion. (a) Left panel:** The procedure for identification of the 'partner-alike genes' to build the expected distributions of correlation coefficients for control, 16p11.2 deletion and duplication carriers. G1, G2 and G3 are genes from 16p11.2 CNV; P1, P2 and P3 are co-expressed interacting partners of G1 from BrainSpan transcriptome; A, C and E are 'partner-alike genes' that are highly co-expressed (Spearman Correlation Coefficient, SCC, ≥0.7) with P1 in controls based on blood transcriptome data. **Upper right panel:** Pairwise SCCs were calculated between G1 and P1 as well as between G1 and all 'P1-alike' genes (A-D) using blood expression profiles from control, 16p11.2 deletion and duplication carriers. **Lower right panel:** The distributions of SCCs between G1 and 'partner-alike genes' in the control (gray line), deletion (red line) and duplication (blue line) carriers as well as SCCs between G1 and P1 in the same datasets (black, red and blue stars, respectively). The deletion and duplication distributions show greater variation among 'partner-alike genes', while the control distribution is less variable. The interacting pairs with altered expression in deletion/duplication carriers were defined as those corresponding to either less than 5th percentile or greater than 95th percentile of the expected distribution of SCCs. In the example above, interacting pair G1-P1 is impacted by the deletion event (SCC is less than 5th percentile of the distribution). The selection of equal

number (*i.e.* 6) of controls, deletion and duplication carriers for this analysis produced similar results. **(b) The distribution of SCCs for KCTD13-CUL3 pair in ten randomly selected sets (6 samples each) of control subjects (multicolored lines), 6 deletion carriers (red line) and 6 duplication carriers (blue line)**. The deletion and duplication distributions show greater variation, while the control distribution is less variable. Although only 10 sets of random controls are shown, the results are similar for one hundred simulations.

## Supplemental Tables

**Table S1. The list of CNVs conferring high risk for four neuropsychiatric disorders, related to Materials and Methods**

CNVs conferring high risk for four neuropsychiatric disorders: ASD (autism spectrum disorders), SCZ (schizophrenia), BD (bipolar disorder), ID (intellectual disability). CNV position, associated disorders, the number of protein-coding genes within each CNV, the number of protein-protein interactions (PPIs) and the number of interacting brain-expressed protein pairs are indicated in the corresponding columns. CNV: copy number variant; PPI: protein-protein interaction

| CNV *locus* | CNV position (Mb) | Psychiatric phenotypes associated with CNV | Protein-Coding Genes | PPIs between brain-expressed genes | | |
|---|---|---|---|---|---|---|
| | | | | # PPIs | # CNV genes | # partners |
| **Combined** | **---** | **---** | 145 | 1,918 | 104 | 1,393 |
| **1q21.1** | 145.0-146.3 | Del: SCZ/ID<br>Dup: ASD/SCZ/BD/ID | 13 | 116 | 6 | 113 |
| **3q29** | 197.2-198.4 | Del: ASD/SCZ/ID | 20 | 253 | 13 | 234 |
| **7q11.23** | 72.4-73.8 | Del: ID<br>Dup: ASD/SCZ/ID | 23 | 330 | 22 | 288 |
| **15q11.2-13.1** | 20.8-26.2 | Del: ASD/SCZ/ID<br>Dup: ASD/SCZ/ID | 14 | 290 | 9 | 264 |
| **16p11.2** | 29.5-30.2 | Del: ASD/ID<br>Dup: ASD/SCZ/BD/ID | 30 | 416 | 21 | 367 |
| **17q12** | 31.9-33.2 | Del: ASD/SCZ/ID | 15 | 261 | 12 | 244 |
| **22q11.21** | 17.1-18.7 | Del: ASD/SCZ/BD/ID<br>Dup: ASD/ID | 30 | 265 | 21 | 234 |

**Table S2. Protein-protein interactions of the 16p11.2 genes (.xlsx file), related to Figure 1**

**Table S3. Developmental brain periods from the BrainSpan** (http://www.brainspan.org), **related to Figure 1**

| Tissue dissection stage | Description | Age | Developmental period |
|---|---|---|---|
| 1 | Early fetal | 8-9 PCW | **P1** |
| 2 | Early fetal | 10-12 PCW | |
| 3 | Early mid-fetal | 13-15 PCW | **P2** |
| 4 | Early mid-fetal | 16-18 PCW | |
| 5 | Late mid-fetal | 19-23 PCW | **P3** |
| 6 | Late fetal | 24-37 PCW | **P4** |
| 7 | Early infancy | 0-5 M | **P5** |
| 8 | Late infancy | 6-11M | |
| 9 | Early childhood | 1-5 Yr | **P6** |
| 10 | Late childhood | 6-11 Yr | |
| 11 | Adolescence | 12-19 Yr | **P7** |
| 12 | Young adulthood | 20-40 Yr | **P8** |

**Table S4. Cell-type specific marker gene enrichment test for four 16p11.2 spatio-temporal networks (P3R1, P3R2, P3R3, P6R2), related to Results**

| Cell type | Marker gene** | Empirical p-value* |
|---|---|---|
| **Astrocyte** | *GFAP, S100B,* ***ALDOC*** | **0.0441** |
| **Cortical GABA interneuron** | *CALB2, CALB1, NOS1, PVALB, CCK, VIP, DLX1, DLX2, NKX2-1, ASCL1, GAD1, GAD2* | NA |
| **Cortical glutamatergic neuron** | *RELN, CUX1, UNC5D, RORB, BCL11B,* ***ETV1****, FEZF2, OTX1,* ***FOXP2****, NTSR1, SOX5, SSTR2, TBR1, TLE4, ZFPM2, CTGF, UNC5C* | **0.0247** |
| **L5 & L6 Cortical glutamatergic neuron** | *ZFPM2, NTSR1, TLE4,* ***FOXP2****, TBR1, SOX5, SSTR2, FEZF2, BCL11B, OTX1,* ***ETV1*** | **0.0098** |
| **L1-L4 Cortical glutamatergic neuron** | *CUX1, UNC5D, RORB, CUX2, SATB2, WFS1, RELN* | NA |
| **Microglia** | *CFH, FCER1G, TNIP2* | NA |
| **Oligodendrocyte** | *CNP, CSPG4, OLIG1, OLIG2, PDGFRA* | NA |

* - empirical p-value was calculated using 10,000 permutations of 187 genes from $HI_{BE}$

** - marker genes in bold are present among 187 partners from our four spatio-temporal networks

Values in bold font indicate statistically significant result (P<0.05)

**Table S5. Interaction patterns of 16p11.2 CNV proteins across networks from different brain regions of the same developmental period and the results of the ANOVA test, related to Figure 4**

Interaction patterns of 16p11.2 CNV proteins across networks from different brain regions (R1: parietal, temporal and occipital cortex; R2: somatosensory, motor and prefrontal cortex; R3: hippocampus, amygdala and striatum) of the same developmental period (P3: late mid-fetal) and the results of the ANOVA test. Bold font indicates the P-value from the ANOVA test (Not significant).

| CNV genes | | Interacting partners in P3R1, P3R2 and P3R3 | | | | | | | |
|---|---|---|---|---|---|---|---|---|---|
| Entrez gene ID | Official symbol | Total partners | Unique to 1 network | | Shared by 2 networks | | Shared by all 3 networks | |
| | | | Count | Freq | Count | Freq | Count | Freq |
| 5595 | MAPK3 | 57 | 21 | 0.368 | 22 | 0.386 | 14 | 0.246 |
| 5531 | PPP4C | 32 | 5 | 0.156 | 8 | 0.250 | 19 | 0.594 |
| 226 | ALDOA | 18 | 6 | 0.333 | 6 | 0.333 | 6 | 0.333 |
| 8479 | HIRIP3 | 17 | 7 | 0.412 | 4 | 0.235 | 6 | 0.353 |
| 9961 | MVP | 10 | 5 | 0.500 | 2 | 0.200 | 3 | 0.300 |
| 10423 | CDIPT | 9 | 1 | 0.111 | 5 | 0.556 | 3 | 0.333 |
| 11151 | CORO1A | 9 | 4 | 0.444 | 5 | 0.556 | 0 | 0 |
| 253980 | KCTD13 | 7 | 3 | 0.429 | 2 | 0.286 | 2 | 0.286 |
| 4150 | MAZ | 6 | 2 | 0.333 | 4 | 0.667 | 0 | 0 |
| 283899 | INO80E | 5 | 5 | 1 | 0 | 0 | 0 | 0 |
| 26470 | SEZ6L2 | 4 | 0 | 0 | 4 | 1 | 0 | 0 |
| 83719 | YPEL3 | 4 | 0 | 0 | 0 | 0 | 4 | 1 |
| 3835 | KIF22 | 3 | 0 | 0 | 3 | 1 | 0 | 0 |
| 9344 | TAOK2 | 3 | 2 | 0.667 | 1 | 0.333 | 0 | 0 |

ANOVA Test

Summary

| *Groups*<br>*Frequency of interactors* | *Count* | *Sum* | *Average* | *Variance* |
|---|---|---|---|---|
| Unique to 1 network | 14 | 4.754 | 0.340 | 0.079 |
| Shared by 2 networks | 14 | 5.801 | 0.414 | 0.098 |
| Shared by all 3 networks | 14 | 3.445 | 0.246 | 0.083 |

Result

| *Source of Variation* | *SS* | *df* | *MS* | *F* | ***P-value*** | *F crit* |
|---|---|---|---|---|---|---|
| Between Groups | 0.199 | 2 | 0.100 | 1.150 | **0.327** | 3.238 |
| Within Groups | 3.378 | 39 | 0.087 | | | |
| | | | | | | |
| Total | 3.577 | 41 | | | | |

**Table S6. Interaction patterns of 16p11.2 CNV proteins across networks from different developmental periods of the same brain region and the results of the ANOVA test, related to Figure 4**

Interaction patterns of 16p11.2 CNV proteins across networks from different developmental periods (P3: late mid-fetal; P6: childhood) of the same brain region (R2: somatosensory, motor and prefrontal cortex) and the results of the ANOVA test. Bold font indicates the statistical significant result (P-value<0.05)

| CNV genes | | Interacting partners in P3R2 and P6R2 | | | | |
|---|---|---|---|---|---|---|
| Entrez gene ID | Official symbol | Total partners | Unique to 1 network | | Shared by 2 networks | |
| | | | Count | Freq | Count | Freq |
| 5595 | MAPK3 | 52 | 33 | 0.635 | 19 | 0.365 |
| 5531 | PPP4C | 29 | 21 | 0.724 | 8 | 0.276 |
| 226 | ALDOA | 18 | 12 | 0.667 | 6 | 0.333 |
| 8479 | HIRIP3 | 10 | 10 | 1 | 0 | 0 |
| 10423 | CDIPT | 9 | 6 | 0.667 | 3 | 0.333 |
| 11151 | CORO1A | 9 | 5 | 0.556 | 4 | 0.444 |
| 9961 | MVP | 7 | 7 | 1 | 0 | 0 |
| 253980 | KCTD13 | 4 | 3 | 0.750 | 1 | 0.250 |
| 4150 | MAZ | 4 | 4 | 1 | 0 | 0 |
| 26470 | SEZ6L2 | 4 | 4 | 1 | 0 | 0 |
| 83719 | YPEL3 | 4 | 1 | 0.250 | 3 | 0.750 |
| 3835 | KIF22 | 3 | 3 | 1 | 0 | 0 |
| 8448 | DOC2A | 2 | 1 | 0.500 | 1 | 0.500 |
| 283899 | INO80E | 2 | 2 | 1 | 0 | 0 |
| 9344 | TAOK2 | 2 | 2 | 1 | 0 | 0 |

ANOVA Test

Summary

| *Groups*<br>*Frequency of interactors* | *Count* | *Sum* | *Average* | *Variance* |
|---|---|---|---|---|
| Unique in 1 network | 15 | 11.748 | 0.783 | 0.057 |
| Shared by 2 networks | 15 | 3.252 | 0.217 | 0.057 |

Result

| *Source of Variation* | *SS* | *df* | *MS* | *F* | ***P-value*** | *F crit* |
|---|---|---|---|---|---|---|
| Between Groups | 2.406 | 1 | 2.406 | 42.143 | **$4.925 \times 10^{-7}$** | 4.196 |
| Within Groups | 1.598 | 28 | 0.057 | | | |
| Total | 4.004 | 29 | | | | |

**Table S7. Enrichment analyses of 16p11.2 spatio-temporal networks in *de novo* mutations, post-synaptic density genes and FRMP target genes (.xlsx file), related to Results**

**Table S8. Pairwise Spearman Correlation Coefficients calculated for *KCTD13*, *CUL3* and *RHOA* using cortical substructures and layers of laser-microdissected (LMD) prenatal human brain (.xlsx file), related to Figure 5**

**Table S9. Co-expressed interacting pairs from four spatio-temporal 16p11.2 networks with altered expression in 16p11.2 CNV deletion and duplication carriers, related to Discussion**

| 16p11.2 gene | Co-expressed interacting partner | SCC | Percentile in background (<5th or >95th) | CNV type |
|---|---|---|---|---|
| MAPK3 | HTRA2 | -0.706 | 1.4th | Del |
| MAPK3 | GAB2 | -0.595 | 2.4th | Del |
| KCTD13 | CUL3 | -0.554 | 2.7th | Del |
| HIRIP3 | CSNK2A2 | -0.963 | 3.7th | Del |
| HIRIP3 | RANBP3 | -0.952 | 4.4th | Del |
| MAPK3 | UBC | 0.554 | 95.9th | Del |
| MAPK3 | DUSP4 | 0.675 | 96.5th | Del |
| HIRIP3 | GART | 0.955 | 98.4th | Del |
| MAPK3 | PPP2CA | -0.933 | 1.3th | Dup |
| MAPK3 | USO1 | -0.639 | 2.0th | Dup |
| MAPK3 | DUSP3 | 0.026 | 3.8th | Dup |
| CDIPT | RTN3 | 0.567 | 95.3th | Dup |
| ALDOA | PCNA | 0.962 | 96.4th | Dup |
| MAPK3 | ID2 | 0.381 | 97.9th | Dup |
| ALDOA | CUL2 | 0.978 | 98.1th | Dup |
| MVP | ZBTB32 | 0.683 | 99.0th | Dup |

## Supplemental Experimental Procedures

### *Control networks and CNV simulation*

Three control datasets have been used to perform statistical comparisons: (1) $HI_{BE}$ served as a background control for comparison with spatio-temporal PPI networks (a total of 116,147 pairs); (2) The dataset of physically interacting brain-expressed human protein pairs from $HI_{BE}$, restricted to the pairs of 1,431 genes from 2,825 common CNVs identified by the 1000 Genomes Consortium (Mills *et al.*, 2011) downloaded from the Database of Genomic Variants (DGV) (MacDonald *et al.*, 2014) (a total of 13,928 pairs); (3) The pairs between brain-expressed 16p11.2 CNV genes and all brain-expressed human genes (a total of 701,112 pairs). Control 1 was used as background in the analysis of spatio-temporal co-expression signatures from high-risk CNVs for **Figure 2**. Controls 1, 2 and 3 were used in the analyses in **Figure 3**. Fisher's exact test was used to calculate statistical significance for comparison between 27 spatio-temporal and control networks. P-values were then FDR-corrected for multiple comparisons.

To further address biases that may be present due to network topology, a permutation strategy was used to randomly simulate CNVs and construct additional control datasets. 10,000 control networks were generated based on the simulated CNVs by randomly selecting genomic regions with the same number of consecutive genes and similar number (±10% variation) of interacting partners from $HI_{BE}$ as in real CNVs. In each iteration, a separate network was built for each of the 10,000 simulated CNVs, and co-expression enrichment analysis was performed across all 27 spatio-temporal networks. Empirical p-values were calculated based on the fraction of 10,000 putative networks with gene pair co-expression frequencies equal or higher than in the real CNV networks. When simulating combined CNV networks for **Figure 2**, the simulations were performed for individual CNVs, and then merged to construct the simulated

combined CNV network. The permutation was performed for 10,000 iterations to create 10,000 simulated combined CNV networks.

***The analysis of physical interactions of wild type and mutant CUL3***

Physical direct interactions of the wild-type and two mutant CUL3 proteins (c.736 G>T, p.Glu246Stop (E246X) and c.1636 C>T, p.Arg546Stop (R546X); reference sequences NM003590 and NP003581) with their corresponding interacting partners were compared using a yeast-two-hybrid system (Y2H) (Dreze *et al.*, 2010). Mutant versions of *CUL3* were generated using site-directed mutagenesis as described (Zhong *et al.*, 2009). Briefly, the wild-type *CUL3* gene from ORFeome 8.1 collection (BC039598, clone ID 5784147; http://horfdb.dfci.harvard.edu/) (Yang *et al.*, 2011) was cloned into the pDEST-AD vector and used as a template for introducing mutations identified in the patients. The mutation-specific primers were as follows: CTAGAATTAATGAAGAAATATAACGAGTGATGCACTGCCTTGA (F) and AGGCAGTGCATCACTCGTTATATTTCTTCATTAATTCTAGCTTC (R) for cloning E246X CUL3; TACTTAGCCAAACACAGTGGTTGACAGCTCACACTCCAGCA (F) and GCTGGAGTGTGAGCTGTCAACCACTGTGTTTGGCTAAGTAGA (R) for cloning R546X *CUL3*.

Two independent PCR reactions were performed using a mutation-specific primer and a vector-specific primer: the primer pairs Tag1-AD forward and mutant reverse were used to introduce the mutation and to amplify the 5' end of the gene until ~20 nucleotides after the mutation position, and the mutant forward/Tag2-Term primers were used to introduce the mutation and amplify starting from ~20 nucleotides before the mutation position until the 3'end. PCR products were used as template for the third stitch-PCR using the primers Tag1 forward and Tag2 reverse. Standard PCR conditions and Platinum® Taq High Fidelity DNA Polymerase (Life Technologies) were used for all PCRs. The vector-specific primers were as follows: GGCAGACGTGCCTCACTACTCGCGTTTGGAATCACTACAGGG (Tag1-AD) and CTGAGCTTGACGCATTGCTAGGAGACTTGACCAAACCTCTGGCG (Tag2-Term). The

merging primers were as follows: GGCAGACGTGCCTCACTACT (Tag1) and CTGAGCTTGACGCATTGCTA (Tag2).

The amplified fragments containing the mutations were introduced into the Gateway entry vector pDONR223 using BP recombination enzyme (Life Technologies) and transformed into the DH5-alpha cells. After growth, single colonies were picked and cultured overnight, plasmid minipreps were then performed to obtain the entry clones with the mutant variants of *CUL3*. All single clones were Sanger sequenced to confirm the presence of the mutation at the desired position and the absence of additional changes.

Each entry clone corresponding to wild-type and mutant *CUL3* variants was sub-cloned into the Gateway pDEST-DB vector via an LR reaction (Life Technologies). Plasmids were subsequently transformed into DH5-alpha cells, and colonies were picked, grown and the plasmids were purified. Then, the plasmids were transformed into the yeast strain Y8930 as previously described (Dreze *et al.*, 2010). The pDEST-AD of the interacting partners (KCTD13, KCTD10, KCTD6, and KCTD9) in the yeast strain Y8800 were picked from the ORFeome 7 collection and the Y2H experiments were performed as previously described (Charloteaux *et al.*, 2011; Dreze *et al.*, 2010). In brief, fresh cultures of all yeast strains DB-CUL3 and AD-partners were grown in SC-Leu and SC-Trp media, respectively, for 2 days at 30°C. Five µL of each culture were spotted on top of each other on YEPD agar plate and grown overnight at 30°C for mating. Diploid selection was performed by replica-plating of cells to SC-Leu-Trp plates and grown at 30°C. After two days, diploid cells were replicated on phenotyping plates 3-AT (control for interaction) and 3-AT with cycloheximide (CHX) (control for autoactivation) and grown for five days at 30°C. Growth on 3-AT plates but not in 3-AT CHX plates indicates activation of the reporter through Y2H interactions. The intensity growth between the wild-type and the mutants was compared to determine the presence or the absence of interaction perturbations. All Y2H experiments were performed in triplicate from different inoculations. Finally, the DB-CUL3 and

AD-partner PCR products amplified from the grown positive colonies were Sanger sequenced to confirm the identities of the interacting partners.

***The analysis of the 16p11.2 CNV transcriptome data from the patients***

To identify interacting protein pairs that are highly co-expressed with the 16p11.2 CNV proteins in the deletions or duplication carriers, we used the expression dataset GSE37772 from GEO. This dataset consists of gene expression profiles of lymphoblast cell lines (LCLs) of autism patients from the Simons Simplex Collection (SSC) generated by Luo *et al.* (Luo *et al.*, 2012). To reduce the noise, only the probes with evidence of robust expression (detection p value ≤ 0.05 in at least 50% of 439 samples) were used. After filtering, 11,171 probes (corresponding to 9,541 genes) were left for the analyses. Our study was carried out on 146 samples: six probands with the 16p11.2 deletion, six probands with the 16p11.2 duplication, and 134 healthy control siblings without 16p11.2 events from the entire SSC collection.

For each spatio-temporal network pair, a list of 'partner-alike genes' was compiled by selecting the genes that are highly co-expressed (SCC≥0.7) with each partner of the 16p11.2 gene in the healthy control SSC siblings (**Figure S5**). Then, the expression profiles of the 'partner-alike genes' from the control siblings were compared with the expression profiles of the same 'partner-alike genes' from the 16p11.2 deletion and duplication carriers. The spatio-temporal network pair was considered to have a significantly reduced expression in the deletion carriers, or a significantly increased expression in the duplication carriers if its co-expression correlation coefficient was lower than 5th percentile or higher than 95th percentile of the background distribution of the correlation coefficients for the 'partner-alike genes'. The 16p11.2 pairs with significant expression changes in deletion and duplication carriers are shown in (**Table S9**).

## Supplemental References

Charloteaux, B., Zhong, Q., Dreze, M., Cusick, M.E., Hill, D.E., and Vidal, M. (2011). Protein-protein interactions and networks: forward and reverse edgetics. Methods Mol Biol 759, 197-213.

Dreze, M., Monachello, D., Lurin, C., Cusick, M.E., Hill, D.E., Vidal, M., and Braun, P. (2010). High-quality binary interactome mapping. Methods Enzymol 470, 281-315.

Luo, R., Sanders, S.J., Tian, Y., Voineagu, I., Huang, N., Chu, S.H., Klei, L., Cai, C., Ou, J., Lowe, J.K.*, et al.* (2012). Genome-wide transcriptome profiling reveals the functional impact of rare de novo and recurrent CNVs in autism spectrum disorders. Am J Hum Genet 91, 38-55.

MacDonald, J.R., Ziman, R., Yuen, R.K., Feuk, L., and Scherer, S.W. (2014). The Database of Genomic Variants: a curated collection of structural variation in the human genome. Nucleic Acids Res 42, D986-992.

Mills, R.E., Walter, K., Stewart, C., Handsaker, R.E., Chen, K., Alkan, C., Abyzov, A., Yoon, S.C., Ye, K., Cheetham, R.K.*, et al.* (2011). Mapping copy number variation by population-scale genome sequencing. Nature 470, 59-65.

Yang, X., Boehm, J.S., Salehi-Ashtiani, K., Hao, T., Shen, Y., Lubonja, R., Thomas, S.R., Alkan, O., Bhimdi, T., Green, T.M.*, et al.* (2011). A public genome-scale lentiviral expression library of human ORFs. Nat Methods 8, 659-661.

Zhong, Q., Simonis, N., Li, Q.R., Charloteaux, B., Heuze, F., Klitgord, N., Tam, S., Yu, H., Venkatesan, K., Mou, D.*, et al.* (2009). Edgetic perturbation models of human inherited disorders. Mol Syst Biol 5, 321.